

LL

LBL-35859
UC-404
Preprint



Lawrence Berkeley Laboratory

UNIVERSITY OF CALIFORNIA

Materials Sciences Division

National Center for Electron Microscopy

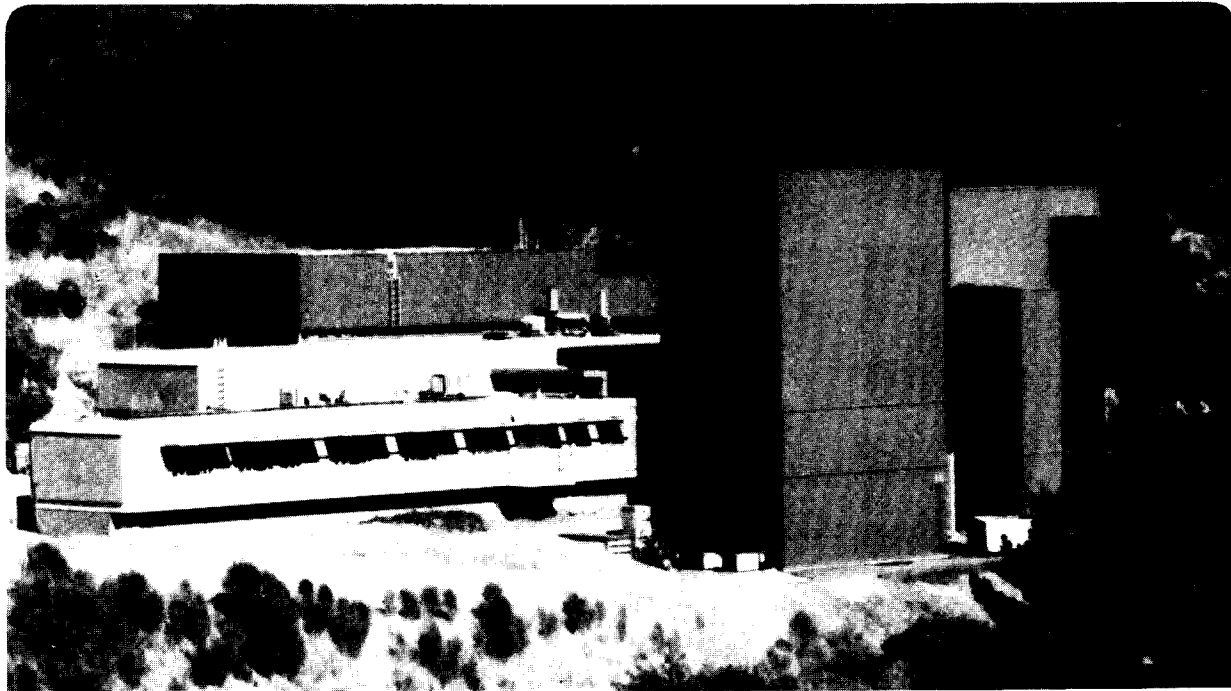
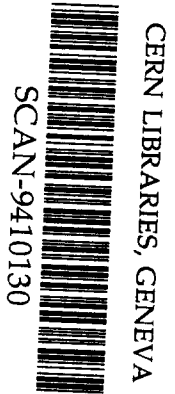
Submitted to Microscopy Research and Technique

sw 9442

Preparation of Oxide Superconductor Specimens for TEM Examination

M. Fendorf, M. Powers, and R. Gronsky

June 1994



Prepared for the U.S. Department of Energy under Contract Number DE-AC03-76SF00098

DISCLAIMER

This document was prepared as an account of work sponsored by the United States Government. Neither the United States Government nor any agency thereof, nor The Regents of the University of California, nor any of their employees, makes any warranty, express or implied, or assumes any legal liability or responsibility for the accuracy, completeness, or usefulness of any information, apparatus, product, or process disclosed, or represents that its use would not infringe privately owned rights. Reference herein to any specific commercial product, process, or service by its trade name, trademark, manufacturer, or otherwise, does not necessarily constitute or imply its endorsement, recommendation, or favoring by the United States Government or any agency thereof, or The Regents of the University of California. The views and opinions of authors expressed herein do not necessarily state or reflect those of the United States Government or any agency thereof or The Regents of the University of California and shall not be used for advertising or product endorsement purposes.

Lawrence Berkeley Laboratory is an equal opportunity employer.

This publication has been reproduced from the best available copy

**Preparation of Oxide Superconductor Specimens
for TEM Examination**

M. Fendorf*, M. Powers*, and R. Gronsky

*Dept. of Chemistry
University of California
Berkeley, CA 94720

*Hewlett-Packard Company
Santa Rosa, CA 95403

Dept. of Materials Sciences & Mineral Eng.
University of California
Berkeley, CA 94720
and
Materials Sciences Division
National Center for Electron Microscopy
Lawrence Berkeley Laboratory
University of California, Berkeley, CA 94720

Microscopy Research and Technique (submitted).

This work was supported in part by the Director, Office of Energy Research, Office of Basic Energy Sciences, Materials Science Division of the U.S. Department of Energy under Contract No. DE-AC03-76SF00098, and by a University of Houston subcontract under DARPA Grant No. MDA972-88-J-1002.



recycled paper

PREPARATION OF OXIDE SUPERCONDUCTOR SPECIMENS FOR TEM EXAMINATION

M. Fendorf¹, M. Powers², and R. Gronsky^{3,4}

¹Department of Chemistry,

University of California, Berkeley, California 94720;

²Hewlett-Packard Company, Santa Rosa, California 95403;

³Department of Materials Science and Mineral Engineering,
University of California, Berkeley, California 94720;

⁴National Center for Electron Microscopy,

Lawrence Berkeley Laboratory, Berkeley, California 94720

TO APPEAR IN:

Microscopy Research and Technique

KEY WORDS:

cleaving, ion beam thinning, ion milling, ultramicrotomy, jet polishing

ABSTRACT

We have investigated a wide variety of oxide superconductors, and report here on a number of techniques that can be effectively used to prepare TEM specimens from these materials. Crushing, cleaving, ion milling, ultramicrotomy, and jet polishing all were successfully utilized, and details of each technique, as well as equipment used, are described. Selection among these methods depends both on the starting form of the material and on the information required. Ion milling and crushing generally give the best results and have the widest applicability in our particular work, while crushing and cleaving involve the least equipment cost. In some cases, particularly with ion milling and jet polishing, small variations in the details of preparation have a dramatic effect on the success rate. We have found it to be a great advantage that the same techniques can be applied in a similar manner to a whole range of oxide materials, even (with some refinements and special precautions) to those which are extremely oxygen or moisture sensitive.

INTRODUCTION

Because of its ability to provide structural images at the atomic level, as well as diffraction and spectroscopic data from extremely small areas, transmission electron microscopy (TEM) is particularly suited to detailed investigations of changes in composition and related defect structures in "high- T_c " and other oxide superconductors. This type of study is essential for understanding the relation between the synthesis, defect content, and macroscopic properties of superconducting materials produced under a range of conditions.

There are now numerous techniques available for thinning solid materials to electron transparency. These include strictly mechanical processes (crushing, cleaving, physical polishing, etc.), chemical and electrochemical techniques (etching, jet polishing, etc.), as well as other, specialized approaches (for example, ion beam thinning and ultramicrotomy). Since the aim of any TEM study is to obtain images which *accurately* represent microstructural features, extreme care in the material thinning process is essential; the choice of an appropriate specimen preparation technique and due attention to all steps involved in applying the technique are both needed in order to avoid the introduction of artifacts which can lead to incorrect conclusions. The effects of the specimen preparation process must be carefully considered, keeping in mind potential changes in not only microstructure but also chemical composition. These should be evaluated against the initial physical form of the sample as well as the type of investigation to be carried out. For bulk superconducting oxides in pellet form, all of the methods mentioned above can be used. However, when the starting material is a powder only crushing and microtomy are applicable, while for thin films ion milling -- and possibly jet polishing -- are the available choices; a summary of specimen preparation approaches applicable to different material forms is given in Table 1. Earlier

publications by Zandbergen *et al.* [1988] and Gu *et al.* [1993] have dealt specifically with preparation of Y-Ba-Cu-O specimens; the present work is intended to review some of the important points presented there, and to extend the discussion to additional materials and techniques.

FABRICATION OF SUPERCONDUCTING MATERIALS

We have carried out TEM studies of superconducting oxides falling into the Y-Ba-Cu-O, Bi-Ca-Sr-Cu-O, La_2CuO_4 , BaBiO_3 , LaCoO_3 , and LiNbO_2 "families".¹ Bulk materials were initially prepared by means of solid state reaction from binary precursors (Y-Ba-Cu-O, Bi-Ca-Sr-Cu-O, LaCoO_3 , LiNbO_2) and by precipitation from molten hydroxide solutions (Y-Ba-Cu-O, La_2CuO_4 , BaBiO_3). For example, in the Y-Ba-Cu-O system, homogeneous, single-phase $\text{YBa}_2\text{Cu}_4\text{O}_8$ (1-2-4) material was fabricated by sintering a stoichiometric mixture of Y_2O_3 , BaO , and CuO for 15 hours at 900°C under an oxygen pressure of 200 bar [Chandrachood *et al.* 1990; see also Karpinski *et al.* 1988]. This material was then re-ground, compacted, and annealed for an additional 15 hours under the same conditions. X-ray diffraction of the resulting material displayed sharp peaks corresponding to the c-spacing of the 1-2-4 structure, confirming that the synthesis was successful. The related compound $\text{Y}_2\text{Ba}_4\text{Cu}_7\text{O}_{15}$ (2-4-7) is produced at more moderate oxygen pressures, <20 bar [Morris *et al.* 1989]. Preparation of $\text{YBa}_2\text{Cu}_3\text{O}_7$ (1-2-3) [see for example Cava *et al.* 1987; Schneemeyer *et al.* 1987; Horowitz *et al.* 1989; Reissner *et al.* 1990], as well as Bi-Ca-Sr-Cu-O materials [Chu *et al.* 1988; Subramanian *et al.* 1988], was carried out in a similar manner, but at atmospheric pressure. We also prepared the 1-2-4 phase at atmospheric pressure using nitrate precursors; in this case, Na_2CO_3 was added to decrease reaction times [Cava *et al.* 1989]. Doped $\text{LaCoO}_{3-\delta}$ and $\text{BaInO}_{3-\delta}$ perovskites

¹ The "dash" notation is used rather than a chemical formula in cases where two or more distinct superconducting phases with different stoichiometries but related crystal structures can occur. Referring to a specific specimen, this notation indicates that a mixture of such phases is present.

were obtained by standard ceramic processing of oxide powders, and also by use of nitrate precursors [Adler *et al.* 1994]. LiNbO_2 and related materials were made by solid-state synthesis in evacuated, sealed tubes at elevated temperatures [Geselbracht *et al.* 1990; Rzeznik *et al.* 1993]. A typical liquid phase synthesis [Ham *et al.* 1988; Marquez *et al.* 1993a; Marquez 1993b] was that of $(\text{La,Nd})_{2-x}(\text{Na,K})_x\text{CuO}_4$, which can be thought of as doped La_2CuO_4 . In this case, La_2O_3 , Nd_2O_3 and CuO are dissolved in equimolar amounts of NaOH and KOH and reacted at 350°C for approximately 20 hours in a silver crucible, until a black, crystalline precipitate forms [Stoll 1993].

Thin films investigated in the present study were exclusively of the Y-Ba-Cu-O type, but the discussion and methods presented here apply equally well to other superconducting films of interest for applications (primarily Bi-Ca-Sr-Cu-O and Tl-Ba-Ca-Cu-O). Three different film geometries were treated; the first was nominally c-axis $\text{YBa}_2\text{Cu}_3\text{O}_7$ on (100)-oriented MgO and $(1\bar{1}02)$ -oriented alumina (Al_2O_3) substrates. In this case, deposition was carried out using laser ablation at 200mTorr oxygen pressure and a substrate temperature of 750°C . A buffer layer of approximately 100\AA CaTiO_3 or SrTiO_3 was deposited on the alumina substrates before growth of the superconductor film was initiated, and the Y-Ba-Cu-O layers were typically 3000\AA thick [Char *et al.* 1990; Tidjani *et al.* 1991].

The other two thin film structures examined were a-axis and c-axis Ag/Y-Ba-Cu-O contacts fabricated using *in-situ*, off-axis sputtering [Sandstrom *et al.* 1988; Eom *et al.* 1990; Newman *et al.* 1990] For this process, a composite Y-Ba-Cu-O target was positioned perpendicular to the substrate surface, and an Ag target parallel to the substrate surface. These films were deposited on (100)- LaAlO_3 and (100) yttria-stabilized zirconia (ZrO_2) substrates, with nominal Ag and Y-Ba-Cu-O layer thicknesses in the range of $800\text{-}1000\text{\AA}$, based on sputtering yield calculations. The c-axis structures were grown with the substrate maintained at 735°C throughout the Y-Ba-Cu-O and Ag deposition steps, while the a-axis orientation resulted from

holding the substrate at 640°C for Y-Ba-Cu-O sputtering and then turning the heater off during Ag sputtering [Powers 1992].

ELECTRON MICROSCOPY

High-resolution TEM imaging was carried out using four instruments: the Berkeley Atomic Resolution Microscope operating at 800kV (1.6Å point-to-point resolution in lattice images), a Hitachi *H-9000NAR* operating at 300kV (1.8Å resolution), a Topcon *002B* operating at 200kV (1.8Å resolution), and a JEOL *JEM200CX* also operating at 200kV (2.3Å resolution). Conventional TEM work, including convergent beam electron diffraction (CBED) and energy-dispersive x-ray spectroscopy (EDS), was performed on a Philips *EM400* operating at 100kV and equipped with a Kevex *Quantum* x-ray spectrometer system. Under an 800kV beam (with LaB₆ filament) Y-Ba-Cu-O specimens are unstable, with observable damage sometimes occurring even during the short time (~1 minute) that a through-focus series of micrographs can be exposed. Occasionally, specimens are rendered completely amorphous during the time of observation. In contrast, damage rates under 200keV and 300keV electron beams are normally negligible, indicating that the energy transferred to atoms in the specimen from electrons at these lower accelerating voltages is below the knock-on (nuclear displacement) threshold for Y-Ba-Cu-O [Merkle *et al.* 1983; Egerton *et al.* 1987]. Other superconducting oxides were observed to exhibit similar behavior, with the exception of BaBiO₃, which damaged rapidly under a 100kV beam and was not imaged at higher accelerating voltages.

PREPARATION OF SPECIMENS FOR TEM EXAMINATION

Crushing and Grinding

The simplest and most rapid specimen preparation method applicable to oxides consists of crushing a small amount of the starting material to a fine powder in an agate mortar. An ordinary sintered alumina mortar is unsuitable, as contamination of the specimen with alumina particles almost always occurs. Best results were obtained by carrying out the crushing with the material submerged in a liquid. It is important to choose a fluid which evaporates easily, will not leave a residue on the specimen surface, and will not react with the superconducting oxide in any way; both ethanol and methanol were used for this purpose in the present study. The superconducting oxides tend to be quite moisture sensitive, and this dictates use of a liquid which is as free of water as possible. After crushing, the smallest particles form a suspension which is then transferred to a holey carbon film supported by a mesh TEM grid using a small disposable syringe, clean pipette, or eye dropper. This procedure results in a dispersion of thin flakes on the grid, as illustrated in Figure 1. Some control over the size of particles captured can be achieved by allowing the suspension to sit undisturbed for 30 seconds to 5 minutes (or more). As time passes, the larger, heavier particles settle to the bottom of the mortar and smaller particles can be drawn off from the top of the liquid. Preparation of these specimens is also facilitated by placing a sheet of filter paper under the grid in order to absorb some of the liquid and speed drying. Since the superconducting oxides considered here are all dark in color, the use of filter paper has the added advantage that the amount of material (number of particles) deposited on the grid can be qualitatively gauged by observing the degree of discoloration of the paper under the grid. The type of specimen support grid used is available from a number of suppliers (for example Structure Probe International catalog number 3620C).

Because of relatively weak bonding between layers in the typical superconducting oxide crystal structures (especially in the Bi-Ca-Sr-Cu-O and LiNbO₂ systems), there is a strong tendency for crystals to cleave along (001) planes. Therefore, the crushing process tends to produce flake-like particles which exhibit a preferred [001] orientation. It is also important to keep in mind that since fracture along grain boundaries is likely during crushing, this method is not an ideal choice for imaging grain boundary structures. The crushing process also will occasionally produce rotational misorientations within a single crystallite in layered materials where bonding is almost two-dimensional [Fortunati 1990]. An additional difficulty which can arise during microscopy is beam-induced sputtering of carbon from the support film and subsequent redeposition as a contamination layer on the surface of the superconductor particles being imaged. This leads to degradation (and eventual complete obscuring) of high-resolution images due to the amorphous "background signal", as well as possible inaccuracies in EDS or Electron Energy Loss Spectroscopy (EELS) microanalysis. However, the problem can be minimized with good microscope column vacuum and the use of a cryogenic anti-contamination device ("cold-finger") near the specimen. With the use of such a device, and with proper handling (imaging as soon as possible after specimen preparation) and storage (desiccator or under vacuum) of specimens, the crushing technique typically yields specimens with surfaces which are extremely clean all the way to the thinnest edge. This is demonstrated by the high-resolution image of Figure 2, where the crystalline structure of the superconductor can be seen in very clear detail.

An additional challenge was presented by the layered dichalcogenide NaNbO₂, shown by x-ray diffraction to be essentially isostructural with LiNbO₂ [Meyer and Hoppe 1976a; 1976b]. Because this material decomposes rapidly (beginning after approximately 1 minute) in the presence of oxygen and moisture it is normally stored under argon in a sealed "glove box", and ordinary bench-top handling is not

possible without destroying the crystal structure. We found that specimens for TEM examination could be successfully prepared -- and potential problems with introducing a solvent into the glove box vacuum system avoided -- by wrapping a small vial of NaNbO_2 powder in kitchen-type plastic wrap, double-sealing this in "zip-lock" plastic bags, transferring it to a polypropylene glove bag back-filled with nitrogen, applying the "crush and grind" procedure described above, and then again placing the finished specimen in plastic wrap and doubled zip-lock bags. Once at the microscope, specimen mounting and transfer to the column were carried out as rapidly as possible, and rubber tubing attached to a pressurized cylinder of N_2 was used to maintain a flow of nitrogen over the specimen at all times. In Figure 3, a diffraction pattern from a specimen made via this isolation technique can be compared with one from a specimen prepared in air and placed in the microscope within a few minutes.

Cleaving and Gluing

A related, but often superior, method of specimen preparation for superconducting oxides involves mounting small, but still "macroscopic" particles on a 3mm metal TEM grid with an electrically conducting adhesive, so that thin edges of the material are exposed. This procedure of course requires the starting material to be in the form of a sintered pellet or "macroscopic" crystallites (approximately 0.5mmx1mm in area, or larger). The fragments to be used are produced by either very coarsely crushing the material or by using a sharp blade to cleave flakes from the starting pellet. Specimens with greater thin area available for TEM imaging can be produced by first grinding the material to a thickness of 50-150 μm , and then breaking off shards with a knife or razor blade. A clean, sharp blade which is easily handled is needed for best results. In either case, once particles

of suitable size² have been obtained, a TEM grid is readied by using a toothpick or similar sharpened stick to deposit one or two small dots of adhesive at the desired mounting location. A cleaved flake is then attached to the grid by placing it directly on top of the adhesive. It can be extremely helpful to use a vacuum "tweezer" to transfer flakes to the waiting dabs of adhesive on the grid, as this greatly reduces the chances of damaging these delicate pieces. Note that two or three fragments can be mounted on a single grid, allowing more area to be examined at the microscope before changing specimens. For this technique we have obtained excellent results with a silver-based epoxy, *EPO-TEK™H20E* (Epoxy Technology, Inc.), which before curing is viscous enough to hold particles in place but pliable enough to allow their position to be adjusted slightly on the grid. The grids used are typically copper, with a 1x2mm oval hole or 1mm circular hole; however, other metals such as aluminum, silver, or gold are available and must be employed in certain special cases (for example, EDS analysis of cuprate materials).

The steps involved in the cleaving and gluing procedure are illustrated in Figure 4, and a finished specimen in Figure 5. Compared to the crushing technique described above, this configuration has the advantages of larger continuous material mass and greater thermal contact with the supporting grid, resulting in improved stability of the specimen under the electron beam. Because of the absence of carbon, and complete lack of contact with any chemicals, specimens produced by cleaving will retain extremely clean, unaltered surfaces as long as they are properly handled and stored; as pointed out earlier, this is especially important for high-resolution imaging and for quantitative microanalysis. The cleaving technique will thus in most cases yield the most artifact-free specimens of any available method; however, because of the natural cleavage of a layered oxide, the thin regions of these

² They must be small enough to fit easily on the grid, but large enough to be handled with tweezers. This generally means a size in the range of 1-2mm by 0.5-1mm in area.

specimens are again often found to be oriented near the [001] zone axis. It is also worth noting that cleaving, along with the crushing and grinding procedure previously described, requires no special equipment or facilities, and hence these represent very low-cost approaches to TEM specimen preparation. In cases where the cleaved particles have insufficient electron-transparent area, the specimen can sometimes be salvaged by briefly ion milling at a shallow angle (see next section), *provided that* the particles have been mounted so that the thinnest edges are positioned at the center of the grid.

Ion Beam Thinning

Many TEM studies of layered superconductors seek to reveal information about c-plane stacking; thus, a sufficiently thin specimen which has the [001] direction *perpendicular* to the incident electron beam is often required. In this respect the methods described above can be somewhat limiting. Therefore, we now turn our attention to specimen preparation techniques which do not depend upon the natural cleavage of the material and hence provide access to a wider range of crystallographic orientations.

One useful method of this type is ion beam thinning [Howitt 1984; Goodhew 1985a]. This is essentially a DC sputtering process, where a beam of ions is accelerated through a potential of a few thousand volts (typically 3-6kV) and then directed at the specimen to be thinned. Ions in this energy range penetrate only a very short distance (a few nanometers) into most materials [Robinson 1964; Trillat 1964]. Then, if enough energy is transferred, the ion collisions cause atoms to be ejected from the surface of the specimen, resulting in a gradual thinning process. Argon (Ar^+) ions are most commonly used because the source atoms are readily available in gaseous form (so that a beam can easily be produced), have high enough atomic mass for good sputtering yield, and are chemically inert. Krypton is a heavier atom and thus provides a more efficient sputtering gas (more energy

transferred per collision) [Franks 1978], but is rarely used because its cost is much higher than that of argon. In the present work, argon ion beam thinning was carried out using a Gatan *Dual Ion Mill Model 600*. Both bulk and cross-sectional thin film specimens for TEM were prepared with the machine operating at 5.0 to 5.5 kV and a 15-18° incident angle, followed by a brief (<30 minutes), low-angle (~10°) final thinning at approximately 3.5 kV. To minimize ion beam damage, all milling was done with a cryogenic specimen stage cooled by liquid nitrogen.

Bulk Material

A number of preparatory steps are required before a specimen can be ion beam thinned to achieve electron transparency. First, a high-precision saw with diamond-coated blade is used to section the starting material into pieces roughly 2mmx2mm in area and 250µm to 500µm thick; a Buehler *Isomet Low Speed Saw* as well as a Buehler *Isomet Plus Precision Saw* have both given good results in sectioning sintered pellets and thin films. Next, using a heavy wax such as *Crystalbond 509™* (Aremco Products, Inc.), one of these pieces is attached to a rigid block of metal or glass sized to fit the hand. Following this, a number of grinding and polishing steps are carried out in order to thin the specimen sufficiently to allow ion beam perforation in a reasonable time period (typically 6-12 hours). Although grinding can be successfully accomplished manually using progressively finer grades of alumina or silicon carbide paper (finishing with 4000 grit, <1µm average particle size), a more efficient approach is to use a polishing wheel (in this case a Buehler *Ecomet III Polisher/Grinder*) with the same grades of paper or with equivalent alumina powder or diamond paste. These steps are greatly facilitated by the use of a disc grinder (here, an E.A. Fischione *p/n 660* was employed), which allows the specimen to be ground and polished while mounted directly on a dimpling platform, eliminating the need for an additional handling step. Wafer thickness following manual polishing should be in the range of 50-75µm. Finally, the

thickness in the center of the specimen is further reduced to 15-25 μm using a precision dimple grinder (in the present case an E.A. Fischione *Model 2000 Specimen Prep System*), leaving it ready for ion milling. This step both minimizes ion milling time and confines thinning to the center of the specimen. The final stages of the dimpling process should be done using a low thinning rate ($\sim 1\mu\text{m}/\text{minute}$) and a fine-grit ($1\mu\text{m}$) diamond paste abrasive. Because superconducting oxides can decompose when exposed to water, it is best to use other fluids as lubricants during cutting, grinding, and polishing steps; we have obtained good results using methanol for this purpose. After dimpling, the specimen is carefully removed from the dimpling platform with acetone and then attached to a TEM grid (1x2mm oval or 1mm circular hole), again using a conducting adhesive as described in the previous section, taking care that the specimen is reasonably well centered on the grid and that no portion of the specimen protrudes beyond the outer edge of the grid. As was the case for the cleaving technique, the use of vacuum tweezers can be very useful in this step. Ion milling preparation steps are described in greater detail in the following section.

It is important to note that the microstructure of a superconducting oxide is seen to have a profound effect on ion milling success [Fortunati *et al.* 1989]. With porous materials, ion milling induces significant mechanical damage, even when carried out at liquid nitrogen temperature. Porosity and poorly connected grain structures, clearly visible for example in the Bi-Ca-Sr-Cu-O pellet of Figure 6, result in a thin edge containing numerous holes and large amorphous regions, as shown in Figure 7. Various ion beam parameters were used on such materials, without an appreciable improvement in specimen quality. In contrast, specimens prepared from denser pellets (in this case Y-Ba-Cu-O, Figure 8) which had undergone hot isostatic pressing after the initial sintering were found to have almost no damage after ion milling, as can be seen in Figure 9 where the twinning characteristic of

YBa₂Cu₃O₇ is clearly visible. The improvement can be attributed to a less porous, larger-grained microstructure produced by the additional processing. Even in the best cases, and with the most careful preparation to minimize milling times, an amorphous surface layer will result from ion beam damage during thinning. There is also the possibility of other types of structural changes being introduced during the ion milling process (e.g., production of stacking faults). It is therefore always advisable to prepare a cleaved or crushed specimen from the same material for comparison with the ion milled one. In spite of these difficulties, ion milling has become a very widely used technique (and sometimes the only possible choice) for bulk and especially thin film high-T_c materials [see for example Kogure *et al.* 1988; Shindo *et al.* 1988; Hiraga *et al.* 1989; Eibl 1990; Kijima and Gronsky 1992].

Thin Film Cross-Sections

The most useful images of superconductor thin films are often cross-sectional views showing the superconductor-substrate interface. Preparation of such specimens is similar to the procedure just described for bulk materials, but requires several additional steps before the final ion milling process is possible. Starting with a wafer typically 1cmx1cmx0.5mm, a high-precision saw (as described above) is used to cut 2-2.5mm strips. Next, two of these strips are glued together, film surface-to-film surface, forming a "sandwich". It is highly advisable to also glue at least one similarly sized piece of "scrap" silicon to each side of the original assembly, in order to provide a backing which enhances mechanical stability and aids in centering the specimen; ideally, the sandwich should be constructed so that its final width is 2-3mm. We have obtained our best results using *M-Bond 610* adhesive (Measurements Group, Inc.). This adhesive requires elevated temperatures and pressures in order to cure properly; it is therefore necessary to clamp the sandwich with a small vise (for example, p/n 10.1400 from VCR Group, Inc.) and place in an oven at approximately 150-175°C for 1-2 hours. Following this, the sandwich is

"sliced" into thin sections approximately 0.3-0.5mm thick, each with the glue line running down the center. The geometry of the steps involved is illustrated in Figure 10, and photographs of a dimpled, mounted specimen before and after ion milling are shown in Figure 11.

As was the case for bulk specimens, a disk grinder is used to polish specimens to an overall thickness of 75-100 μ m, and dimpling is necessary before ion beam thinning can begin. We have found that for thin film cross sections the details of the dimpling procedure are critical to the ultimate success of the ion milling process. A thickness of no more than 20 μ m must be reached in the center of the specimen, and results are greatly improved if this is done in stages. Specifically, the dimpling process begins using a 3mm wide "flattening" wheel with 6 μ m-grit diamond paste to reach a thickness of approximately 50 μ m across the full width of the specimen; a dimpling rate of 5 μ m/minute is used at this stage. When this first step is completed, the material thickness at the center of the specimen should be measured with a calibrated optical microscope. Tolerance stack-up makes it difficult to accurately assess specimen thickness mechanically on the dimpling machine, and in fact an accuracy better than $\pm 10\mu$ m probably cannot be achieved with such measurements, which of course causes serious difficulties when a final thickness of no more than 20 μ m is required.

Next, the dimpler is fitted with a "standard" 1mm-wide dimpling wheel and with 1 μ m-grit diamond paste, the specimen is thinned at a rate of 3-5 μ m/minute until the thickness is approximately 25 μ m at the center. At this point, the dimpling rate is reduced to 1 μ m/minute in order to lessen the chances of damaging the specimen. For any thinning below 20 μ m, the rate should be even further decreased, to 0.5 μ m/minute. It is very important to visually check the condition of the specimen many times as dimpling progresses, and in particular it should be inspected about once per minute during the last 5 μ m of thinning. These

examinations are best done using an illuminated, magnifying eyepiece placed directly on the dimpling machine, so that both the specimen and the dimpling platform remain undisturbed. Dimpling must be terminated at the first sign of damage or cracks in the specimen, since once these begin to form during dimpling, chances of successful ion milling are almost nil and further thinning will inevitably cause complete destruction of the specimen. The final specimen configuration achieved using the above procedure is illustrated in Figure 12.

When dimpling is complete, the specimen is removed from the dimpling platform by soaking in acetone and then attached to a TEM grid, just as was described in the preceding section for bulk material. For cross-sectional specimens we recommend the use of grids with a 0.5x2mm slot-type hole, with the slot carefully aligned along the interface line of the specimen. The use of a vacuum tweezer is almost essential, as the dimpled thin-film cross sections are even more fragile than bulk specimens. In addition, the ion milling process itself requires more care for cross-sections than for plan-view or bulk specimens. This is due to different sputtering rates for various materials. The best ion milling results are obtained when the ion beam is approximately perpendicular to the film-substrate interface. We have found that the yield of specimens which are evenly thinned across the interface is significantly improved if the ion mill is fitted with a *sector controller* which ceases or reduces the action of the beam except over a small angular range. A high-resolution TEM image from a finished, successfully ion milled cross-sectional specimen is shown in Figure 13.

Ultramicrotomy

Ultramicrotomy [Goodhew 1985b; Malis and Steele 1990] is another specimen preparation technique which offers ready access to all crystallographic orientations, and has therefore also been used to prepare TEM specimens from superconducting

oxides [Subramanian *et al.* 1988; Matsui *et al.* 1990; Gu *et al.* 1993]. The starting material is first crushed to a powder (if not already in that form) in an agate mortar, and then imbedded in a polymerizing resin contained within a gelatin capsule or plastic mold. After the resin is cured, the resulting block is trimmed to a small cross section ($\sim 0.1\text{mm} \times 0.1\text{mm}$) at one end, and then sliced with a diamond knife blade to yield thin sections. The very thin (electron transparent) sections of resin are then floated onto fine-mesh TEM grids (again, using a liquid *other than* water) and allowed to dry. Under ideal circumstances, the embedded superconductor particles are cut along a variety of crystallographic directions. A significant difficulty of this technique is to produce sections thin enough for TEM examination without causing the imbedded particles to disintegrate or to separate from the resin. For microtomy of oxide superconductors, *LR White*[®] "hard" grade resin (London Resin Co.) was found to give the best results, with minimal pull-out and tearing problems [see Csencsits *et al.* 1985; Csencsits and Gronsky 1988]. A 2-hour cure at 95°C ($\pm 2^\circ\text{C}$) was used to polymerize the resin. The microtome employed was an RMC *MT-6000* utilizing a 55° diamond knife blade. A cutting rate of $1\text{mm}/\text{second}$ yielded good quality thin sections, which were captured on 400-mesh copper grids. Stability under an electron beam was improved by evaporating a thin layer of carbon ($<100\text{\AA}$) onto the surface of completed specimens.

An example of a specimen produced by ultramicrotomy is shown in Figure 14. We were able to obtain conventional TEM images in many different crystallographic orientations from microtomed specimens, but discovered that it is not usually possible to retain oxide particles within the resin when sections are sliced thin enough ($<\sim 300\text{\AA}$) for high-resolution imaging. Section thicknesses actually achieved are more typically in the range of $500\text{-}1000\text{\AA}$; these exhibit a characteristic gold to silver-gray color. Microtomed specimens also show some deformation in the direction of knife travel. In spite of these drawbacks, the full range of

orientations provided by ultramicrotomy make it worthwhile for some materials science investigations. This technique is a particularly attractive choice in analytical studies where compositional information is to be obtained, since uniform section thickness is extremely important for quantitative EDS, CBED, and EELS work [Williams 1984; Goldstein and Williams 1986; Isaacson 1993].

Jet Polishing

This is an electrochemical thinning technique which minimizes artifacts due to mechanical handling of the specimen and also yields thin areas in all crystallographic orientations. For the oxides considered here, we have chosen to use a non-acid electrolyte which has been shown to be effective in jet polishing a wide variety of materials [Kestel 1986; 1988]. The solution, known as *BK-2*, is prepared by adding 5.30g (0.125 moles) LiCl, 16.56g (0.05 moles) $Mg(ClO_4)_2 \cdot 6H_2O$, and 100ml of 2-butoxyethanol (also known as butyl cellosolve, ethylene glycol monobutyl ether, or butyl glycol) to 500ml of methanol. Note that the hydrated magnesium perchlorate was chosen so that additional water uptake during weighing and handling would be minimized. Also, all of the components of the solution are hazardous; in particular, 2-butoxyethanol is a reproductive toxin and magnesium perchlorate is a strong oxidizer. Therefore, it is important to handle these chemicals with care (inside an operating fume hood, and wearing appropriate hand and eye protection).

To begin the preparation process, specimens roughly 2x2mm in area and 150-250 μ m thick were cut from a sintered pellet of $YBa_2Cu_4O_8$ with a low-speed saw using an ultra thin, diamond-coated blade. The clamping mechanism in most jet polishing machines is designed to accept 3mm circular specimens, and if desired such discs can be punched from the wafered material using an ultrasonic disc cutter (e.g., Gatan Model 601). Whether or not the ultrasonic cutter is used, the final

specimen for jet polishing is ground to a thickness of approximately 100 μm using a disc grinder and 2400 grit or finer abrasive paper, or a polishing wheel, as described in the *Ion Milling* section. Specimens prepared in our study ranged in thickness from 90 to 120 μm after this step. Most of the small wafers were then further thinned by dimpling with 1 μm diamond paste until a final thickness of 75 μm in the central area was reached. Finally, jet polishing was carried out at a potential of 150V, using an E.A. Fischione *Model 130 Digital Power Control*.

During polishing, the electrolyte was maintained at a temperature between -55°C and -65°C; this was achieved by pre-cooling the solution to approximately -40°C in a methanol refrigeration unit (FTS Systems *Multi-Cool*) and then briefly placing the vessel containing the solution in a liquid nitrogen bath. Upon termination of polishing, specimens were immediately rinsed in two successive baths of pure methanol. Under the conditions described here, thinning is quite rapid, with perforation occurring in less than 30 seconds. This makes monitoring for the optimal stopping point difficult, and many specimens were over-etched. The polishing rate and total polishing time could possibly be made more manageable by using thicker starting specimens (~150 μm) and somewhat less LiCl and Mg(ClO₄)₂ in the electrolyte solution.

Temperature control is also extremely important, and we have found in earlier trials that temperatures which are too high lead to contamination of the specimen in the form of small, spherical surface deposits (as illustrated in Figure 15), while temperatures which are too low cause the electrolyte viscosity to increase to the point where polishing is not possible. Nevertheless, we did have success with the jet polishing technique, and it offers the advantage that once the apparatus is set up and the electrolyte mixed, a number of specimens can be prepared very rapidly. A TEM image of a completed specimen with satisfactory thin area and no discernible surface deposits is shown in Figure 16.

SELECTION OF METHOD

As mentioned in the introduction, the physical form of the material to be examined is a primary consideration in choosing a TEM specimen preparation technique. However, it is also apparent from the discussion presented in the preceding sections that several other important factors cannot be overlooked in deciding on the best approach. These include changes in microstructure, chemical alteration (e.g. surface contamination), accessibility of pertinent features and crystallographic orientation, cost of necessary equipment, and to a lesser extent, the level of expertise and training needed as well as time and labor involved in producing a specimen.

When absolute cleanliness and lack of alteration of the material are of paramount importance, crushing or cleaving should be first choices, as they cause minimal changes to the microstructure of brittle oxides in most cases, and produce regions thin enough for good quality high-resolution images. In addition, these techniques, along with ultramicrotomy, cause no chemical change or surface contamination when properly carried out. When very accurate, quantitative microanalysis is required, ultramicrotomy has the further advantage of a uniform section thickness, but the disadvantage that specimens usually must be coated with carbon for stability. In contrast, jet polishing can be expected to chemically alter the specimen, at least in a surface layer, and therefore is not a preferred method when compositional information is needed. No chemical changes *per se* generally are produced in ion milled specimens, but microstructural artifacts are a definite possibility, and in most cases an amorphous surface layer will be present (which can present a problem for high-resolution imaging).

The drawback of the crushing and cleaving approaches is that they offer limited availability of certain crystallographic orientations and little selectivity over which

portions of the original material are made electron transparent. Therefore, when these are decisive factors in a study -- when specimen areas with [001] perpendicular to the beam direction must be maximized, when grain boundaries are the features of interest, etc. -- ion milling, ultramicrotomy, or jet polishing are the best options. When a number of specimens for conventional TEM imaging are needed, for example to investigate variations in microstructure throughout a sintered pellet, jet polishing is particularly attractive, since it allows rapid, consistent thinning over many runs and thins all crystallographic orientations equally. Microtomy and jet-polishing are less successful than ion milling for the production of specimens for high-resolution imaging, due to the difficulty in obtaining sufficiently thin areas.

Preservation of a very specific interface (e.g., bicrystals, thin film cross-sections) necessitates the use of ion milling, with jet polishing or ultramicrotomy a possibility in some cases. In such studies it must be kept in mind that specimens can suffer microcracking during mechanical polishing steps, and these cracks can later be filled with re-deposited, amorphous material during ion thinning, resulting in possible misleading images of the microstructure.

From the points above, it should be clear that a decision must be made as to which one or two factors is most important in a particular TEM study. This, along with the starting configuration of the material, will determine the most appropriate specimen preparation technique(s). In our own work, most investigations were carried out on powders and thin films, and many involved lattice imaging, so crushing and ion milling were the specimen preparation techniques we found to be most useful. Finally, in spite of all other considerations, cost and availability of equipment can sometimes play a role in determining which specimen technique is used. Jet polishing, ultramicrotomy, and especially ion milling equipment costs are rather high (\$10K-\$100K), while crushing and cleaving involve virtually no investment (<\$100). Successful application of ion milling and ultramicrotomy

techniques also require a significant level of user skill, making prior training by an experienced operator a necessity.

ACKNOWLEDGMENTS

We wish to express our thanks to M. Chandramouli, J.-B. Liu, B. Simion, J. Ulan, R. Wilson and J. Van Slyke for technical assistance and helpful discussions, as well as to K. Fortunati and M. Tidjani for early inspiration toward this paper. We also gratefully acknowledge the Texas Center for Superconductivity at the University of Houston (TCSUH), Morris Research, Inc., Conductus, Inc., and the A.M. Stacy Group at U.C. Berkeley for supplying samples used in this study. Our appreciation is extended to Nissei Sangyo America, Inc. for kindly providing a Hitachi *H-9000NAR* microscope to the University of California. Portions of the TEM work were performed at the National Center for Electron Microscopy, Lawrence Berkeley Laboratory, a facility funded by the Director, Office of Energy Research, Office of Basic Energy Sciences, Materials Sciences Division of the U.S. Department of Energy under Contract Number DE-AC03-76SF00098. This work was supported in part by a University of Houston subcontract under DARPA Grant. No. MDA972-88-J-1002. Mention of any commercial product in this paper does not constitute an endorsement by the University of California, by Lawrence Berkeley Laboratory, by the U.S. Department of Energy, or by Hewlett-Packard Company.

REFERENCES

- Adler, S., Russek, S., Reimer, J., Fendorf, M., Stacy, A., Huang, Q., Santoro, A., Lynn, J., Baltisberger, J., and Werner, U. (1994) Local Structure and Oxide-Ion Motion in Defective Perovskites. *Solid State Ionics*, in press.
- Cava, R.J., Batlogg, B., van Dover, R.B., Murphy, D.W., Sunshine, S., Siegrist, T., Remeika, J.P., Reitman, E.A., Zahurak, S., and Espinosa, G.P. (1987) Bulk Superconductivity at 91K in Single-Phase Oxygen-Deficient Perovskite $\text{YBa}_2\text{Cu}_3\text{O}_{7-\delta}$. *Phys. Rev. Lett.* **58**, 1676-1679.
- Cava, R.J., Krajewski, J.J., Peck, W.F., Batlogg, B., Rupp, L.W., Fleming, R.M., James, A.C.W.P., and Marsh, P. (1989) Synthesis of Bulk Superconducting $\text{YBa}_2\text{Cu}_4\text{O}_8$ at One Atmosphere Pressure. *Nature* **338**, 328-330.
- Chandrachood, M.R., Morris, D.E., and Sinha, A.P.B. (1990) Phase Diagram and New Phases in the Y-Ba-Cu-O System. *Physica C* **171**, 187-193.
- Char, K., Newman, N., Garrison, S.M., Barton, R.W., Taber, R.C., Laderman, S.S., and Jacowitz, R.D. (1990) Microwave Surface Resistance of Epitaxial $\text{YBa}_2\text{Cu}_3\text{O}_7$ Thin Films of Sapphire. *Appl. Phys. Lett.* **57**, 409-411.
- Chu, C.W., Bechtold, J., Gao, L., Hor, P.H., Huang, Z.J., Meng, R.L., Sun, Y.Y., Wang, Y.Q., and Xue Y.Y. (1988) Superconductivity up to 114K in the Bi-Al-Ca-Sr-Cu-O Compound System without Rare-Earth Elements. *Phys. Rev. Lett.* **60**, 941-943.
- Csencsits, R., Schooley, C., and Gronsky, R. (1985) An Improved Method for Thin Sectioning of Particulate Catalysts. *J. Electr. Microsc. Tech.* **2**, 643-644.
- Csencsits, R. and Gronsky, R. (1988) Preparation of Zeolites for TEM Using Microtomy. In: *Specimen Preparation for Transmission Electron Microscopy of Materials*, J.C. Bravman, R.M. Anderson, and M.L. McDonald, eds., Materials Research Society, Pittsburgh, MRS Symp. Proc. **115**, 103-108.
- Egerton, R.F., Crozier, P.A., and Rice, P. (1987) Electron Energy-Loss Spectroscopy and Chemical Change. *Ultramicroscopy* **23**, 305-312.
- Eibl, O. (1990) Crystal Defects in $\text{Bi}_2\text{Sr}_2\text{Ca}_{n-1}\text{Cu}_n\text{O}_{4+2\delta}$ Ceramics. *Physica C* **168**, 249-256.
- Eom, C.B., Sun, J.Z., Lairson, B.M., Streiffer, S.K., Marshall, A.F., Yamamoto, K., Laderman, S.S., Taber, R.C., and Jacowitz, D. (1990). Synthesis and Properties of $\text{YBa}_2\text{Cu}_3\text{O}_7$ Thin Films Grown Insitu by 90-Degrees Off-Axis Single Magnetron Sputtering. *Physica C* **171**, 354-382.

- Fortunati, K., Fendorf, M., Powers, M., Burmester, C.P., and Gronsky, R. (1989) Preparation of BiCaSrCuO Specimens for High-Resolution Transmission Electron Microscopy. In: *Proceedings of the 47th Annual Meeting of the Electron Microscopy Society of America*, G.W. Bailey, ed., San Francisco Press, San Francisco, pp. 714-715.
- Fortunati, K. (1990) Electron Microscopy of Transition-Metal Doped BiCaSrCuO Superconductors. Thesis, University of California, Berkeley, pp. 19-21.
- Franks, J. (1978) Ion Beam Technology and Electron Microscopy. In: *Advances in Electronics and Electron Physics*, vol. 47, L. Marton, ed., Academic Press, New York, pp. 13-20.
- Geselbracht, M.J., Richardson, T.J., and Stacy, A.M. (1990) Superconductivity in the Layered Compound Li_xNbO_2 . *Nature* 354, 324-326.
- Goldstein, J.I. and Williams, D.B. (1986) Quantitative X-Ray Analysis. In: *Principles of Analytical Electron Microscopy*, D.C. Joy, A.D. Romig, and J.I. Goldstein, eds., Plenum Press, New York, pp. 180-183.
- Goodhew, P.J. (1985a) In: *Thin Foil Preparation for Electron Microscopy*, A.M. Glauert, ed., Elsevier Science Publishers, Amsterdam, pp. 103-116.
- Goodhew, P.J. (1985b) In: *Thin Foil Preparation for Electron Microscopy*, A.M. Glauert, ed., Elsevier Science Publishers, Amsterdam, pp. 117-123.
- Gu, H., Ruault, M.O., and Beriot, E. (1993) Comparison of Different TEM Sample Preparation Methods for $\text{YBa}_2\text{Cu}_3\text{O}_{7-\delta}$ Type Materials. *Microscopy, Microanalysis, Microstructures* 4, 51-61.
- Ham, W.K., Holland, G.F., and Stacy, A.M. (1988) Low-Temperature Synthesis of Superconducting $\text{La}_{2-x}\text{M}_x\text{CuO}_4$: Direct Precipitation from NaOH/KOH Melts. *J. Am. Chem. Soc.* 110, 5214-5215.
- Hiraga, K., Oku, T., Shindo, D., and Hirabayashi, M. (1989) High-Resolution Electron Microscopy Study on Crystal Structures of High- T_c Superconductors. *J. Electron Microsc. Tech.* 12, 228-243.
- Horowitz, H.S., Bordia, R.K., Torardi, C.C., Morrisey, K.J., Subramanian, M.A., McCarron, E.M., Michel, J.B., Askew, T.R., Flippen, R.B., Bolt, J.D., and Chowdhry, U. (1989) The Effect of Synthesis Methods on the Processing and Properties of $\text{YBa}_2\text{Cu}_3\text{O}_{6+x}$. *Solid State Ionics* 32/33, 1087-1099.
- Howitt, D.G. (1984) Ion Milling of Materials Science Specimens for Electron Microscopy: A Review. *J. Electron Microsc. Tech.* 1, 405-414.

- Isaacson, M. (1993) Simple Considerations on Microanalysis Using Electron Beams. *Ultramicroscopy* 49, 171-178.
- Karpinski, J., Kaldis, E., Jilek, E., Rusieki, S., and Bucher, B. (1988) Bulk Synthesis of the 81-K Superconductor $\text{YBa}_2\text{Cu}_4\text{O}_8$ at High Oxygen Pressure. *Nature* 336, 660-662.
- Kestel, B.J. (1986) Non-Acid Electrolyte Thins Many Materials for TEM Without Causing Hydride Formation. *Ultramicroscopy* 19, 205-211.
- Kestel, B.J. (1988) Jet Thinning of $\text{YBa}_2\text{Cu}_3\text{O}_x$ High T_c Superconductor and also Gold for TEM with a Non-Acid Electrolyte. *Ultramicroscopy* 25, 351-354.
- Kijima, N., and Gronsky, R. (1992) Crystal Structure of the High- T_c Phase (T_c approximately 111K). *Jpn. J. Appl. Phys. (Part 2 - Letters)* 31, L82-L85.
- Kogure, T., Zhang, Y., Levonmaa, R., Kontra, R., Wang, W.X., Rudman, D.A., Yurek, G.J., and Vander Sande, J.B. (1988) Grain Boundary Structure of $\text{YBa}_2\text{Cu}_3\text{O}_{7-x}$ Formed by Oxidation of Metallic Precursors. *Physica C* 156, 707-716.
- Malis, T.F., and Steele, D. (1990) Ultramicrotomy for Materials Science. In: *Specimen Preparation for Transmission Electron Microscopy of Materials II*, R. Anderson, ed., Materials Research Society, Pittsburgh, MRS Symp. Proc. 199, 3-42.
- Marquez, L.N., Keller, S.W., Stacy, A.M., Fendorf, M., and Gronsky, R. (1993a) Synthesis of Twin-Free, Orthorhombic $\text{EuBa}_2\text{Cu}_3\text{O}_{7-\delta}$ Superconductors at 450°C by Direct Precipitation from Molten NaOH and KOH. *Chemistry of Materials* 5, 761-764.
- Marquez, L.N. (1993b) Synthesis of Copper and Bismuth Oxide Superconductors by Direct Precipitation from Molten Alkali Metal Hydroxides and Nitrates. Thesis, University of California, Berkeley, pp. 41-43.
- Matsui, Y., Takekawa, S., Horiuchi, S., Shoda, K., Umezono, A., Nakamura, S., and Tsuruta, C. (1990) High-Resolution Transmission Electron Microscopy of Modulated Structures and Defects in Bi-Sr-Ca-Cu-O Superconductors Prepared by Various Procedures. *J. Electron Microsc.* 39, 223-230.
- Merkle, K.L., King, W.E., Bailey, A.C., Haga, K., and Meshii, M. (1983) Experimental Determination of the Energy Dependence of Defect Production. *J. Nucl. Materials* 117, 4-11.
- Meyer, G. and Hoppe, R. (1976a) Über Oxoniobate(III): Zur Kenntnis von LiNbO_2 . *J. Less-Common Metals* 46, 55-65.

Meyer, G. and Hoppe, R. (1976b) Notiz zur Kenntnis von NaNbO_2 . Z. Anorg. Allg. Chem. 424, 128-132.

Morris, D.E., Asmar, N.G., Wei, J.Y.T., Nickel, J.H., Sid, R.L., Scott, J.S., and Post, J.E. (1989) Synthesis and Properties of the 2:4:7 Superconductors $\text{R}_2\text{Ba}_4\text{Cu}_7\text{O}_{15-x}$ ($\text{R}=\text{Y, Eu, Gd, Dy, Ho, Er}$). Phys. Rev. B 40, 11406-11409.

Newman, N., Char, K., Garrison, S., Barton, R., Taber, R., Eom, C., Geballe, T., and Wilkens, B. (1990). $\text{YBa}_2\text{Cu}_3\text{O}_{7-\delta}$ Superconducting Films with Low Microwave Surface Resistance Over Large Areas. Appl. Phys. Lett. 57, 520-522.

Powers, M. (1992) High Resolution Transmission Electron Microscopy Study of Ag/YBCO Multilayers for Metal Contact Applications. Thesis, University of California, Berkeley, pp. 13-14.

Reissner, M., Steiner, W., Stroh, R., Hörhager, S., Schmid, W., and Wruss, W. (1990) Influence of Sintering Temperature on the Superconducting Properties of $\text{YBa}_2\text{Cu}_3\text{O}_{7-x}$. Physica C 167, 495-502.

Robinson, M.T., Holmes, D.K., and Oen, O.S. (1964) Monte Carlo Calculations of the Ranges of Energetic Atoms in Solids. In: *Ionic Bombardment, Theory and Applications*, J.J. Trillat, ed., Gordon and Breach Science Publishers, New York, pp. 161-174.

Rzeznik, M.A., Geselbracht, M.J., Thompson, M.S., and Stacy, A.M. (1993). Superconductivity and Phase Separation in Na_xNbO_2 ($x < 1$). Angewandte Chemie International Edition in English 32, 254-255.

Sandstrom, R.L., Gallagher, W.J., Dinger, T.R., Koch, R.H., Laibowitz, R.B., Kleinsasser, W., Gambino, R.J., Bumble, B., and Chisolm, M.F. (1988). Reliable Single-Target Sputtering Process for High-Temperature Superconducting Films and Devices. Appl. Phys. Lett. 53, 444-446.

Schneemeyer, L.F., Wasczak, J.V., Zahorak, S.M., van Dover, S.M., and Siegrist, T. (1987) Superconductivity in Rare Earth Cuprate Perovskites. Mat. Res. Bull. 22, 1467-1473.

Shindo, D., Hiraga, K., Hirabayashi, M., Kikuchi, M., and Syono, Y. (1988) Structure Analysis of High- T_c Superconductor Bi-Ca-Sr-Cu-O by Processing of High-Resolution Electron Microscope Images. Jpn. J. Appl. Phys. 27, L1018-L1021.

Stoll, S.L. (1993) Synthesis, Structure and Properties of Alkali Metal Doped Lanthanum Copper Oxides. Thesis, University of California, Berkeley, pp. 31-60.

Subramanian, M.A., Torardi, C.C., Calabrese, J.C., Gopalakrishnan, J., Morrissey, K.J., Askew, T.R., Flippen, R.B., Chowdhry, U., and Sleight, A.W. (1988) A New High-Temperature Superconductor: $\text{Bi}_2\text{Sr}_{3-x}\text{Ca}_x\text{Cu}_2\text{O}_{8+y}$. *Science* **239**, 1015-1017.

Tidjani, M.E., Gronsky, R., Kingston, J.J., Wellstood, F.C., and Clarke, J. (1991) Heteroepitaxial $\text{YBa}_2\text{Cu}_3\text{O}_{7-x}$ - SrTiO_3 - $\text{YBa}_2\text{Cu}_3\text{O}_{7-x}$ Trilayers Examined by Transmission Electron Microscopy. *Appl. Phys. Lett.* **58**, 765-767.

Trillat, J.J. (1964) Ionic Bombardment, A New Method for the Study of Surfaces. In: *Ionic Bombardment, Theory and Applications*, J.J. Trillat, ed., Gordon and Breach Science Publishers, New York 13-50.

Williams, D.B., (1984) *Practical Analytical Electron Microscopy in Materials Science*, Philips Electronic Instruments Inc, Electron Optics Publishing Group, Mahwah, NJ, pp. 4, 77-81.

Zandbergen, H.W., Hetherington, C., and Gronsky, R. (1988) Sample Preparation of $\text{YBa}_2\text{Cu}_3\text{O}_{7-\delta}$ for High-resolution Electron Microscopy. *J. Supercond.* **1**, 21-34.

TABLE 1
APPLICABLE TEM SPECIMEN PREPARATION
TECHNIQUES FOR DIFFERENT MATERIAL FORMS

<u>MATERIAL FORM</u>	crush	cleave	ion mill	microtome	jet polish
<u>SPECIMEN PREP METHOD</u>					
loose powder	●			●	
sintered pellet	●	●	●	●	●
single crystal	●	●	● (a)		● (a)
thin film			●	● (b)	● (b)

(a) depends on original size
(b) may be possible

FIGURE CAPTIONS

- Figure 1: Low-magnification TEM image of $\text{BaIn}_{1-x}\text{Zr}_x\text{O}_{3-\delta}$ ($x=0.33$) particles supported on holey carbon film, in specimen produced by crushing method.
- Figure 2: High-resolution TEM image from doped La_2CuO_4 specimen prepared by crushing technique. Note the high level of detail and lack of surface contamination at the thinnest edge of the particle.
- Figure 3: Selected area diffraction patterns from NaNbO_2 specimens prepared (A) in glove bag and (B) on open bench top. The hexagonal crystal structure of this material is preserved in the first case, but has notably decomposed in the second.
- Figure 4: Schematic illustration of steps involved in producing TEM specimen by cleaving and gluing technique.
- Figure 5: Optical microscope image of Y-Ba-Cu-O specimen prepared by cleaving and gluing.
- Figure 6: SEM image of porous microstructure in superconducting Bi-Ca-Sr-Cu-O pellet.
- Figure 7: TEM image of ion-milled specimen from material shown in previous figure.
- Figure 8: SEM image of denser $\text{YBa}_2\text{Cu}_3\text{O}_{7-\delta}$ pellet produced by hot isostatic pressing.
- Figure 9: TEM image showing successful ion milling of pellet from previous figure. Light and dark bands representing different twin domains characteristic of the 1-2-3 phase are clearly visible.

Figure 10: Illustration of steps involved in preparation of cross-sectional TEM specimen from thin film material.

Figure 11: Optical microscope images of cross-sectional specimens before (left) and after (right) ion milling.

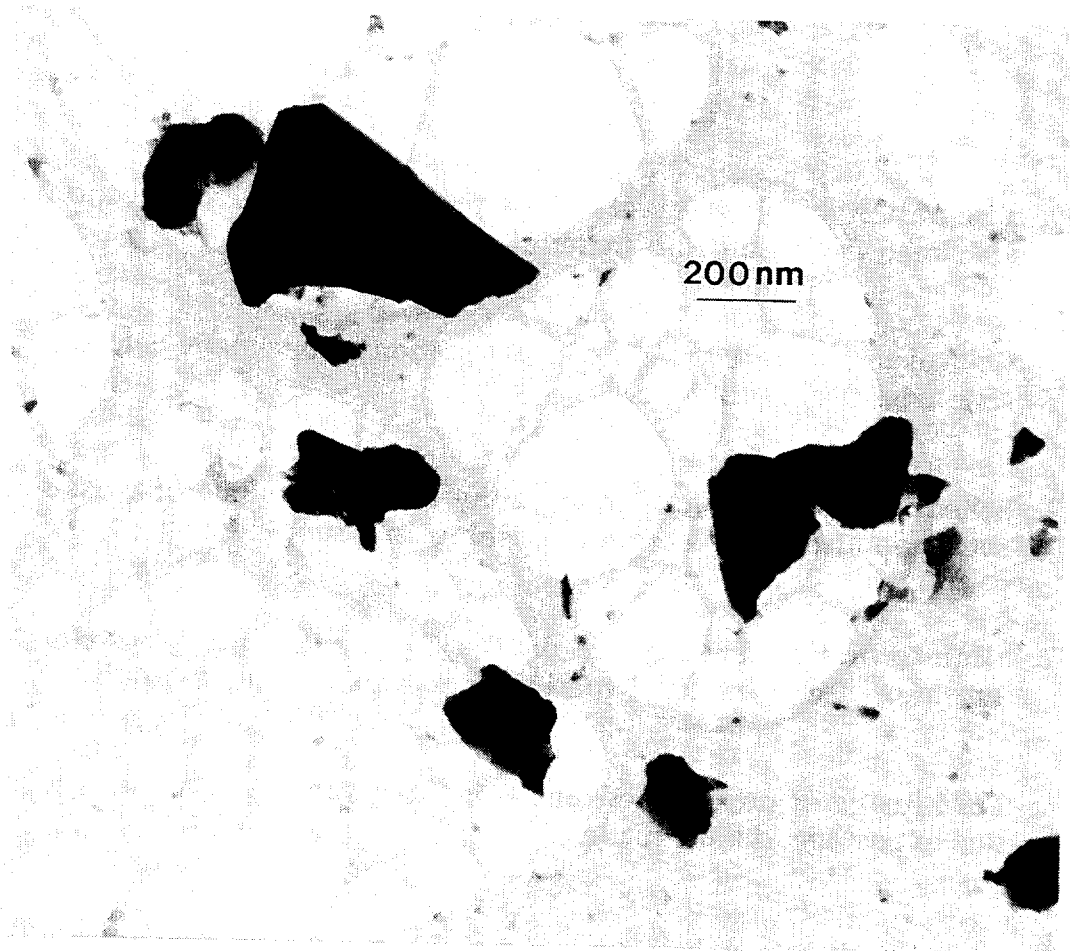
Figure 12: Schematic illustration of topography and dimensions of cross-sectional specimen after completion of polishing and dimpling steps.

Figure 13: High-resolution TEM image of $\text{YBa}_2\text{Cu}_3\text{O}_7$ thin film (YBCO) on MgO substrate. Cross-sectional specimen was produced by ion milling.

Figure 14: TEM image of microtomed Bi-Ca-Sr-Cu-O specimen. Note deformation due to passage of knife blade.

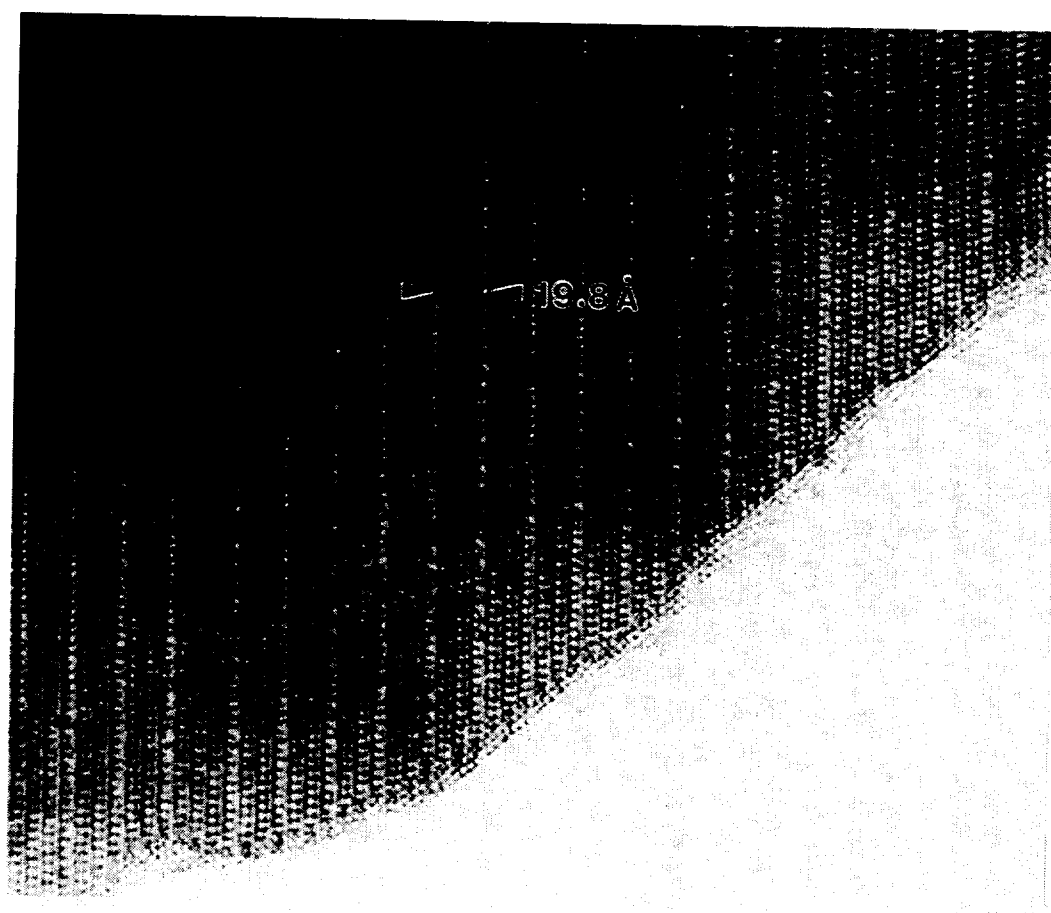
Figure 15: TEM image of Y-Ba-Cu-O specimen jet-polished with inadequate temperature control. Spherical surface deposits are clearly visible.

Figure 16: TEM image of Y-Ba-Cu-O specimen successfully prepared by jet polishing.



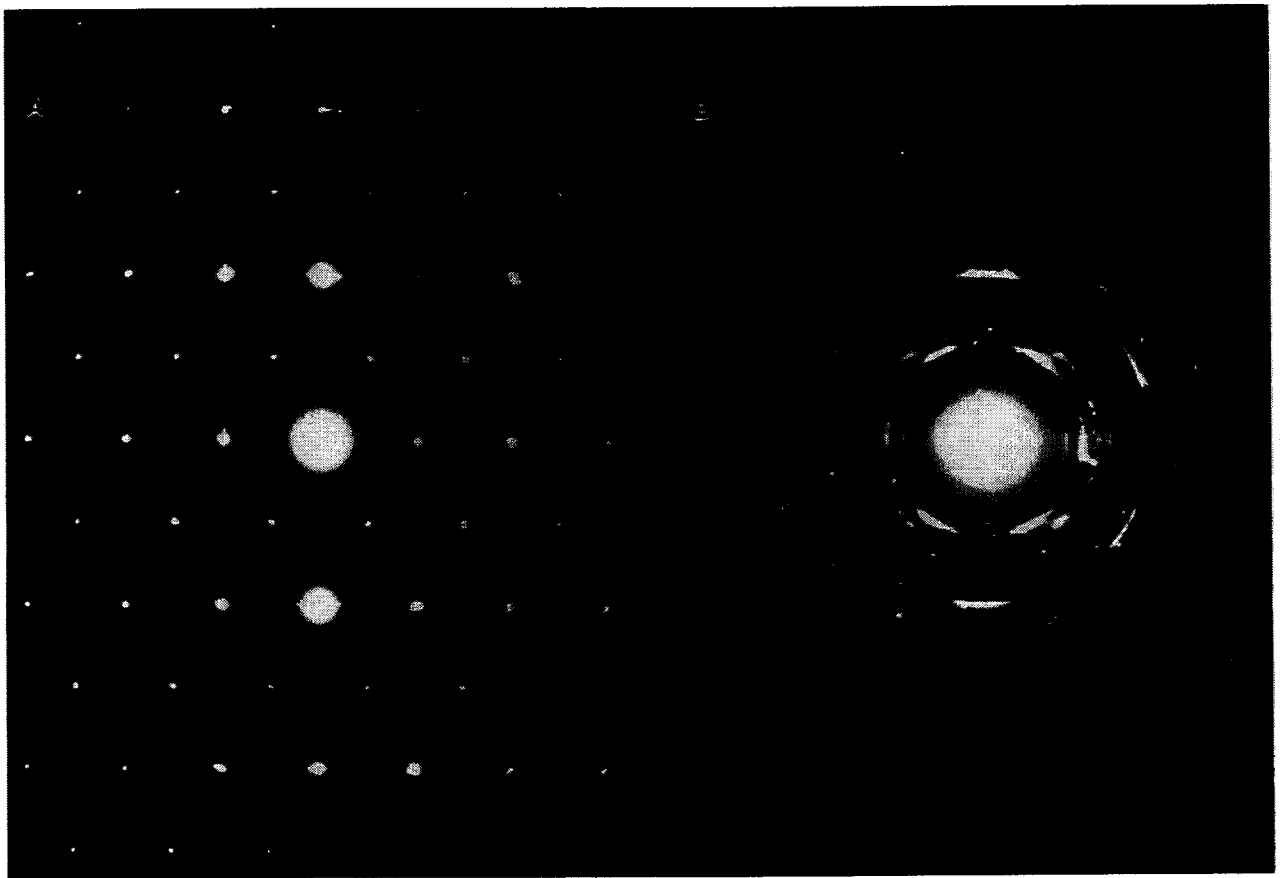
XBB 945-2734

Figure 1



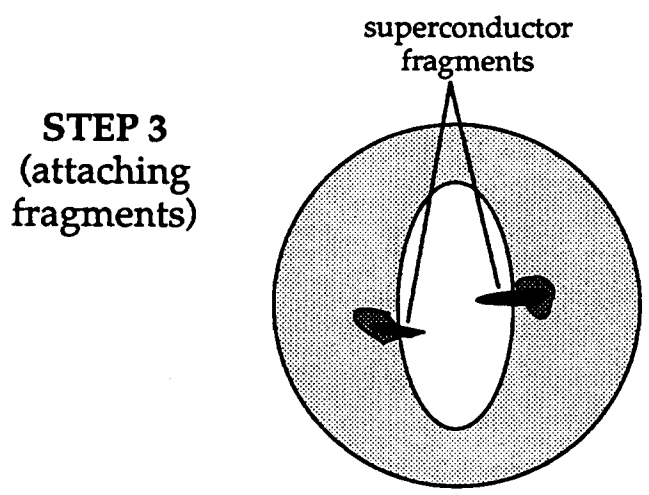
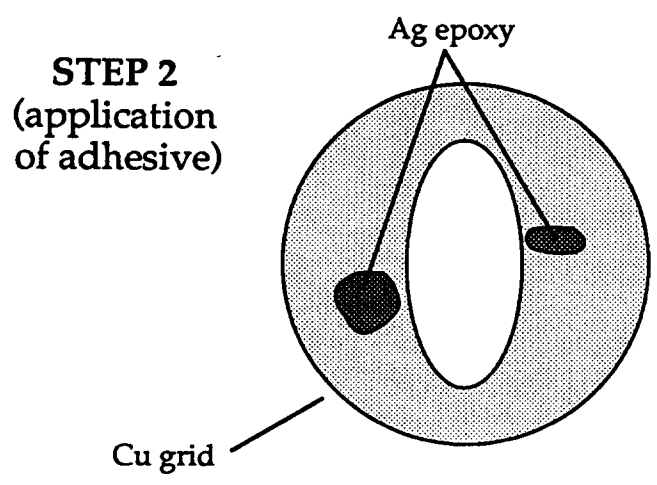
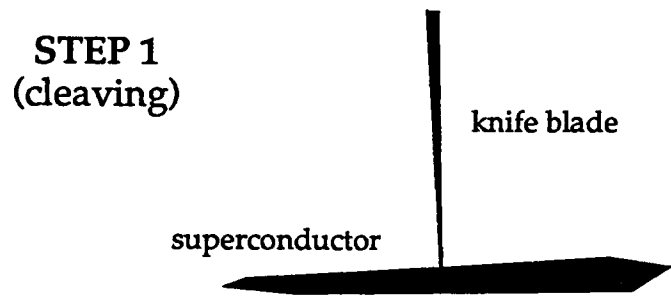
XBB 945-2735

Figure 2



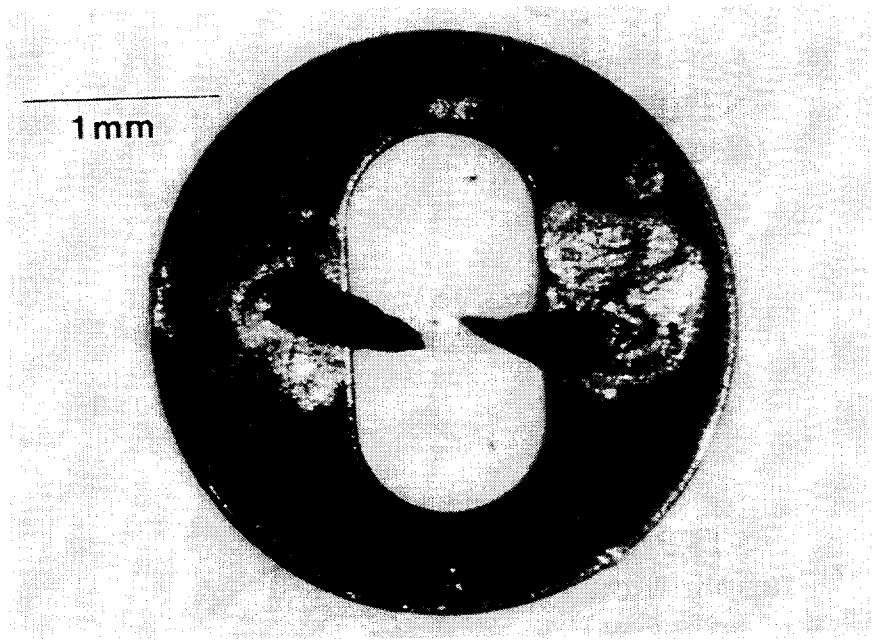
XBB 945-2736

Figure 3



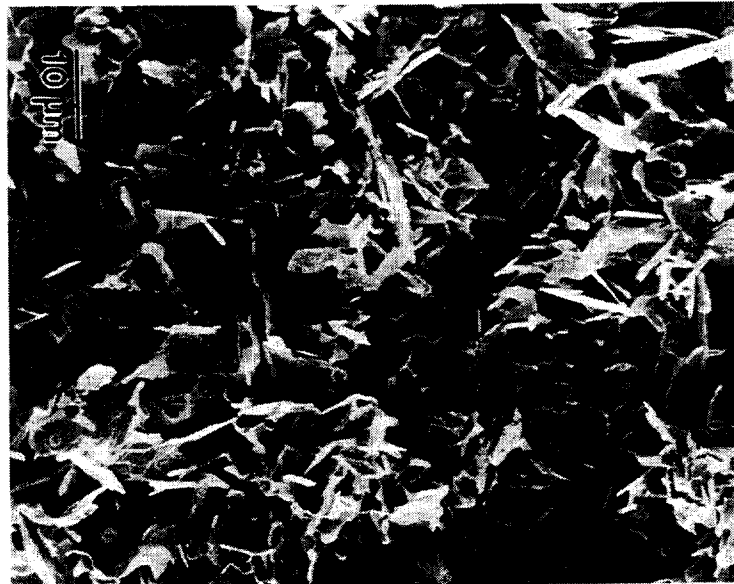
XBL 945-299

Figure 4



XBB 945-2732

Figure 5



XBB 903-2091

Figure 6



XBB 893-1535

Figure 7



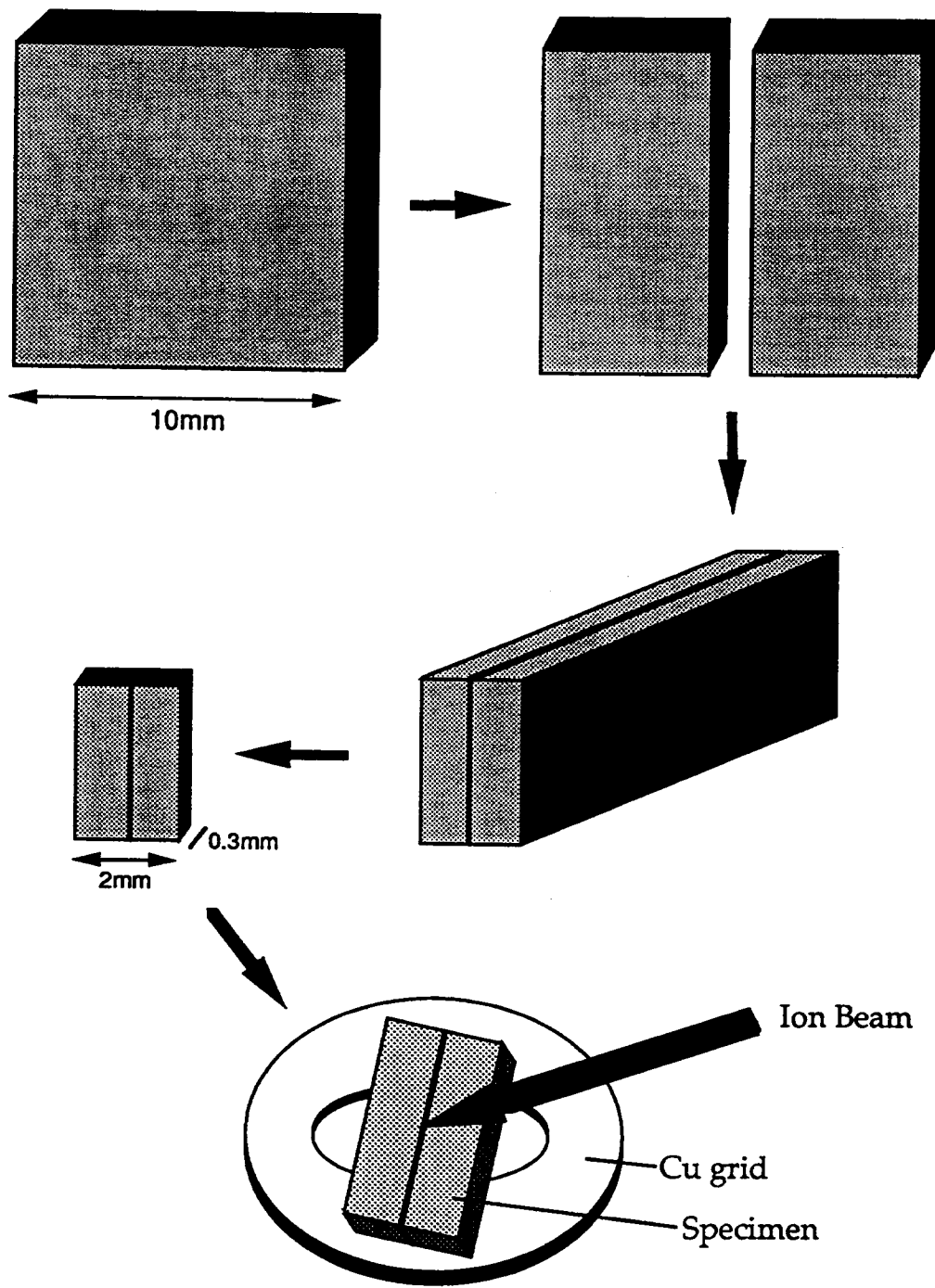
XBB 903-2090

Figure 8



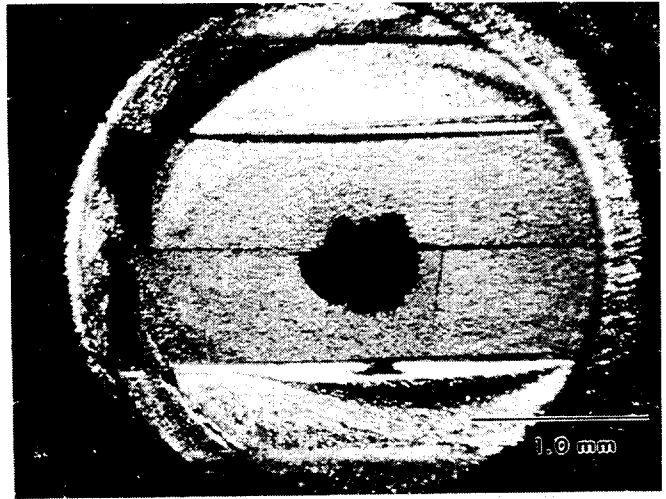
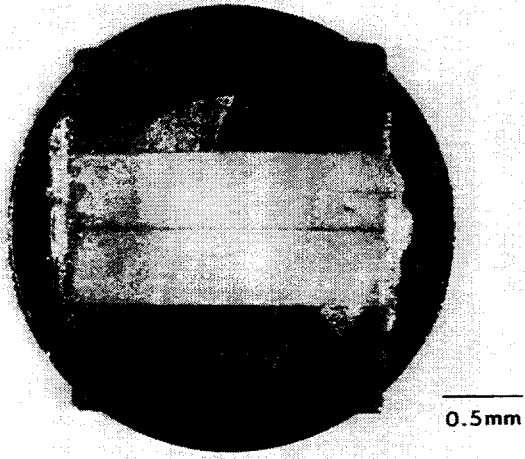
XBB 903-2089

Figure 9



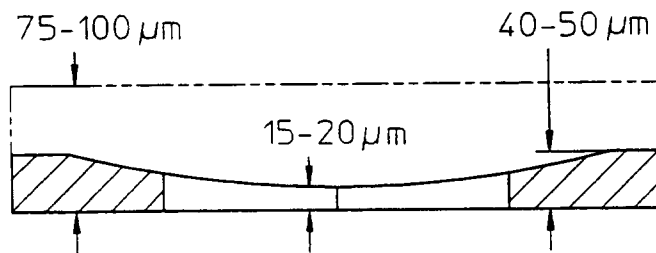
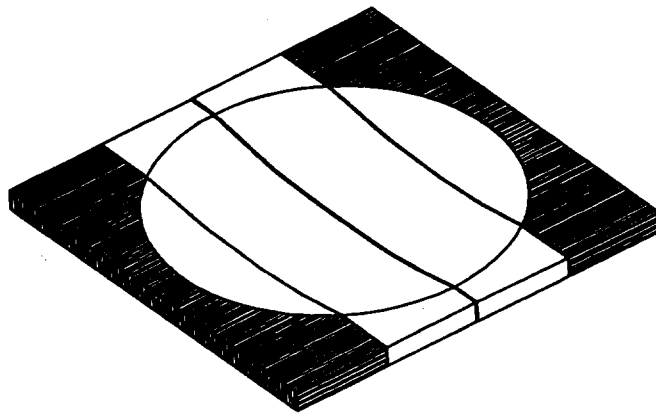
XBL 928-1900

Figure 10



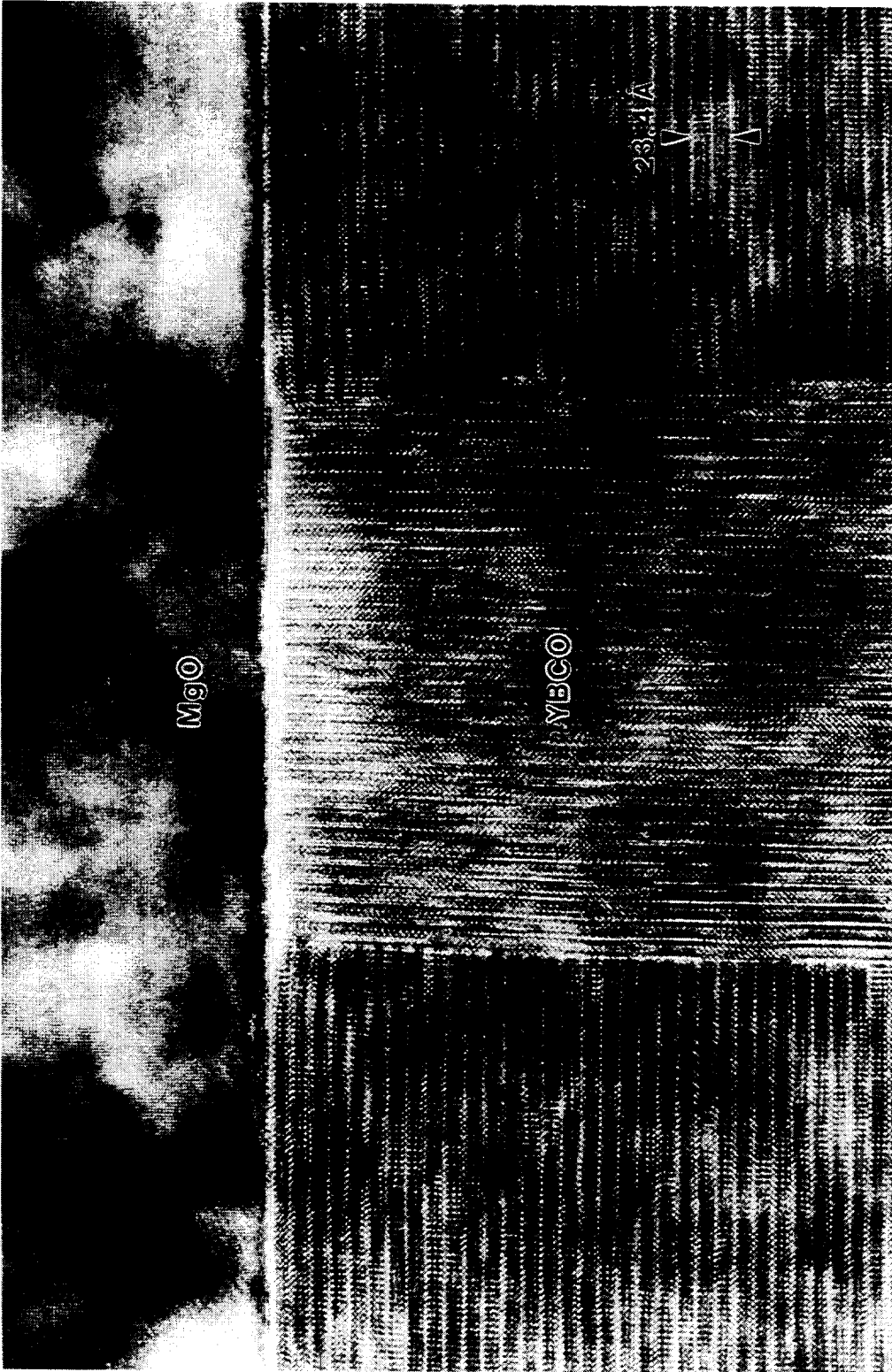
XBB 925-3471

Figure 11



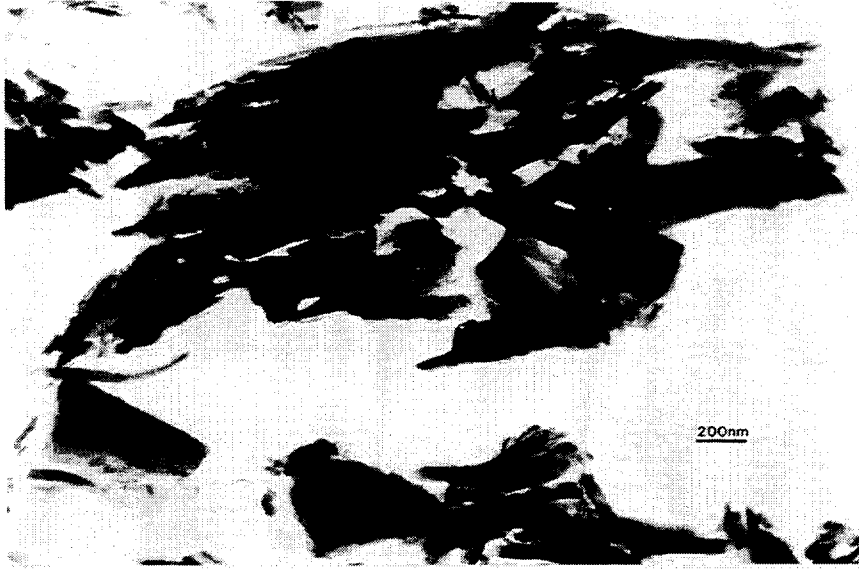
XBL 945-300

Figure 12



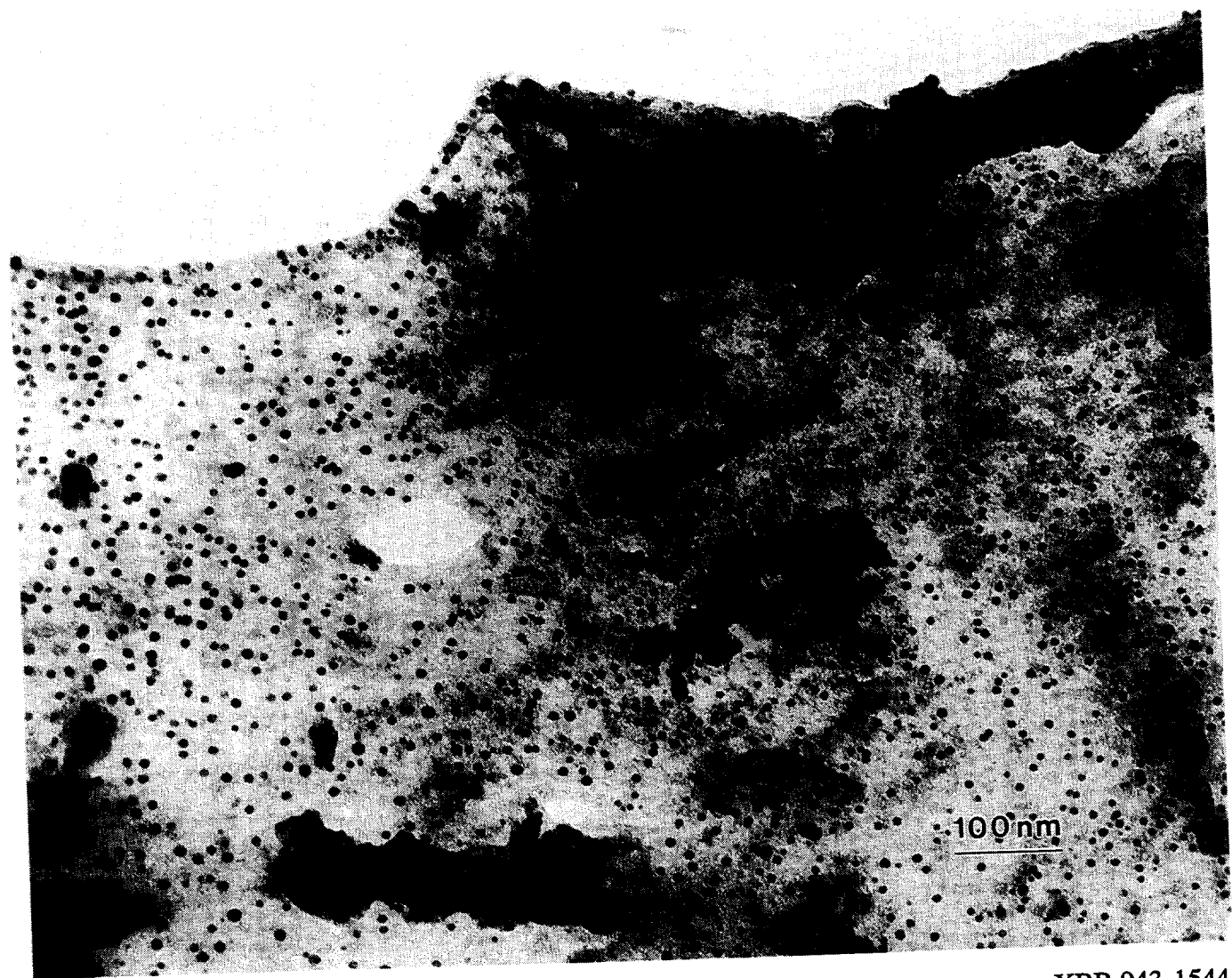
XBB 945-2737

Figure 13



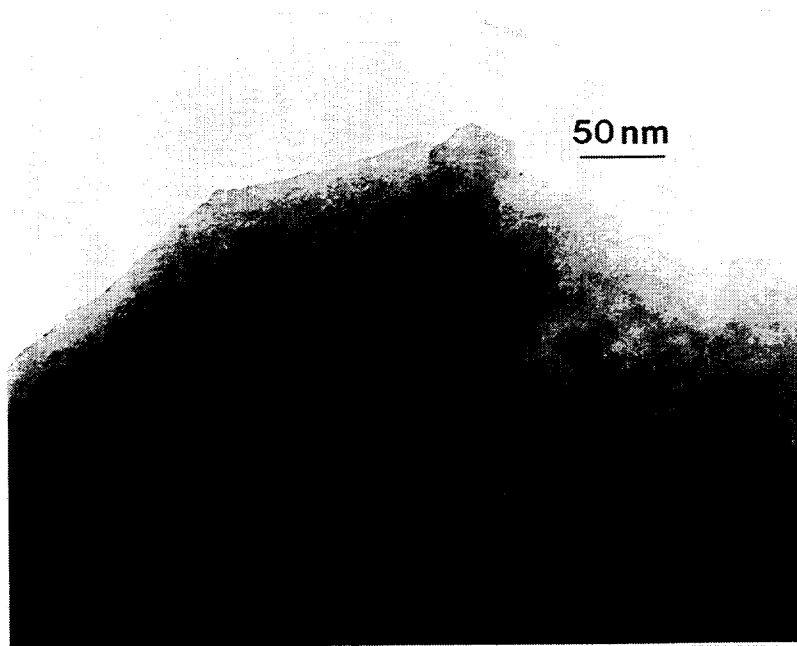
XBB 894-3090C

Figure 14



XBB 943-1544

Figure 15



XBB 945-2733

Figure 16